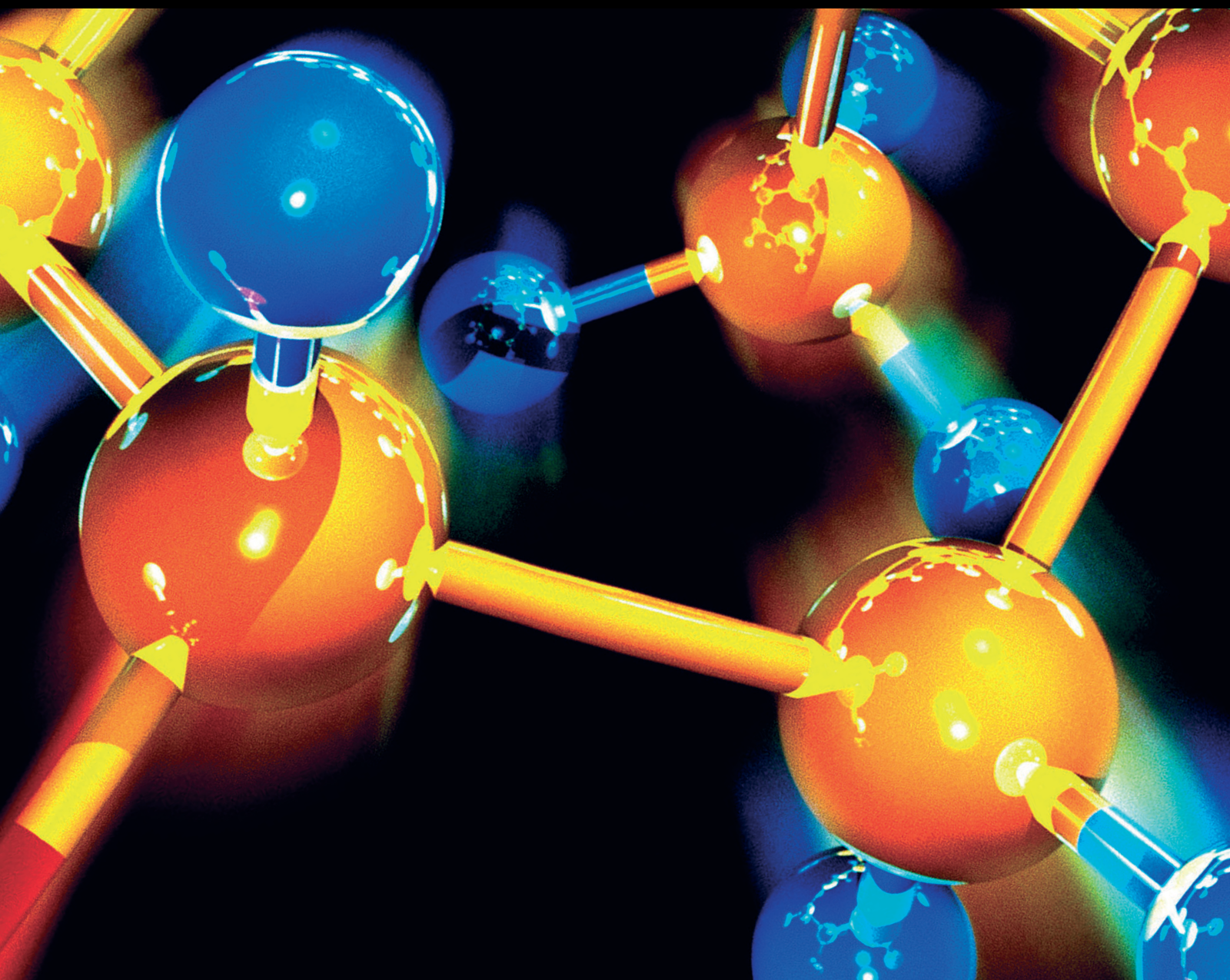


Environmental Magnetism Use in Studying Heavy Metal Contamination

Lead Guest Editor: Stanislav Frančičković-Bilinski

Guest Editors: Sanja Sakan and Tadeusz Magiera





Environmental Magnetism Use in Studying Heavy Metal Contamination

Environmental Magnetism Use in Studying Heavy Metal Contamination



Lead Guest Editor: Stanislav Frančišković-Bilinski

Guest Editors: Sanja Sakan and Tadeusz Magiera

Chief Editor

Kaustubha Mohanty, India

Associate Editors

Mohammad Al-Ghouti, Qatar
Tingyue Gu , USA
Teodorico C. Ramalho , Brazil
Artur M. S. Silva , Portugal

Academic Editors




Jinwei Duan, China
Luqman C. Abdullah , Malaysia
Dr Abhilash , India
Amitava Adhikary, USA
Amitava Adhikary , USA
Mozhgan Afshari, Iran
Daryoush Afzali , Iran
Mahmood Ahmed, Pakistan
Islam Al-Akraa , Egypt
Juan D. Alché , Spain
Gomaa A. M. Ali , Egypt
Mohd Sajid Ali , Saudi Arabia
Shafaqat Ali , Pakistan
Patricia E. Allegretti , Argentina
Marco Anni , Italy
Alessandro Arcovito, Italy
Hassan Arida , Saudi Arabia
Umair Ashraf, Pakistan
Narcis Avarvari , France
Davut Avci , Turkey
Chandra Azad , USA
Mohamed Azaroual, France
Rasha Azzam , Egypt
Hassan Azzazy , Egypt
Renal Backov, France
Suresh Kannan Balasingam , Republic of Korea
Sukanta Bar , USA
Florent Barbault , France
Maurizio Barbieri , Italy
James Barker , United Kingdom
Salvatore Barreca , Italy
Jorge Barros-Velázquez , Spain
THANGAGIRI Baskaran , India
Haci Baykara, Ecuador
Michele Benedetti, Italy
Laurent Billon, France

Marek Biziuk, Poland
Jean-Luc Blin , France
Tomislav Bolanca , Croatia
Ankur Bordoloi , India
Cato Brede , Norway
Leonid Breydo , USA
Wybren J. Buma , The Netherlands
J. O. Caceres , Spain
Patrizia Calaminici , Mexico
Claudio Cameselle , Spain
Joaquin Campos , Spain
Dapeng Cao , China
Domenica Capasso , Italy
Stefano Caporali , Italy
Zenilda Cardeal , Brazil
Angela Cardinali , Italy
Stefano Carli , Italy
Maria F. Carvalho , Portugal
Susana Casal , Portugal
David E. Chavez, USA
Riccardo Chelli , Italy
Zhongfang Chen , Puerto Rico
Vladislav Chrastny , Czech Republic
Roberto Comparelli , Italy
Filomena Conforti , Italy
Luca Conti , Italy
Christophe Coquelet, France
Filomena Corbo , Italy
Jose Corchado , Spain
Maria N. D.S. Cordeiro , Portugal
Claudia Crestini, Italy
Gerald Culioli , France
Nguyen Duc Cuong , Vietnam
Stefano D'Errico , Italy
Matthias D'hooghe , Belgium
Samuel B. Dampare, Ghana
Umashankar Das, Canada
Victor David, Romania
Annalisa De Girolamo, Italy
Antonio De Lucas-Consuegra , Spain
Marccone A. L. De Oliveira , Brazil
Paula G. De Pinho , Portugal
Damião De Sousa , Brazil
Francisco Javier Deive , Spain
Tianlong Deng , China

Fatih Deniz , Turkey
Claudio Di Iaconi, Italy
Irene Dini , Italy
Daniele Dondi, Italy
Yingchao Dong , China
Dennis Douroumis , United Kingdom
John Drexler, USA
Qizhen Du, China
Yuan Yuan Duan , China
Philippe Dugourd, France
Frederic Dumur , France
Grégory Durand , France
Mehmet E. Duru, Turkey
Takayuki Ebata , Japan
Arturo Espinosa Ferao , Spain
Valdemar Esteves , Portugal
Cristina Femoni , Italy
Gang Feng, China
Dieter Fenske, Germany
Jorge F. Fernandez-Sanchez , Spain
Alberto Figoli , Italy
Elena Forte, Italy
Sylvain Franger , France
Emiliano Fratini , Italy
Franco Frau , Italy
Bartolo Gabriele , Italy
Guillaume Galliero , France
Andrea Gambaro , Italy
Vijay Kumar Garlapati, India
James W. Gault , Canada
Barbara Gawdzik , Poland
Pier Luigi Gentili , Italy
Beatrice Giannetta , Italy
Dimosthenis L. Giokas , Greece
Alejandro Giorgetti , Italy
Alexandre Giuliani , France
Elena Gomez , Spain
Yves Grohens, France
Katharina Grupp, Germany
Luis F. Guido , Portugal
Maolin Guo, USA
Wenshan Guo , Australia
Leena Gupta , India
Muhammad J. Habib, USA
Jae Ryang Hahn, Republic of Korea

Christopher G. Hamaker , USA
Ashanul Haque , Saudi Arabia
Yusuke Hara, Japan
Naoki Haraguchi, Japan
Serkos A. Haroutounian , Greece
Rudi Hendra , Indonesia
Javier Hernandez-Borges , Spain
Miguel Herrero, Spain
Mark Hoffmann , USA
Hanmin Huang, China
Doina Humelnicu , Romania
Charlotte Hurel, France
Nenad Ignjatović , Serbia
Ales Imramovsky , Czech Republic
Muhammad Jahangir, Pakistan
Philippe Jeandet , France
Sipak Joyasawal, USA
Sławomir M. Kaczmarek, Poland
Ewa Kaczorek, Poland
Mostafa Khajeh, Iran
Srećko I. Kirin , Croatia
Anton Kokalj , Slovenia
Sevgi Kolaylı , Turkey
Takeshi Kondo , Japan
Christos Kordulis, Greece
Ioannis D. Kostas , Greece
Yiannis Kourkoutas , Greece
Henryk Kozłowski, Poland
Yoshihiro Kudo , Japan
Avvaru Praveen Kumar , Ethiopia
Dhanaji Lade, USA
Isabel Lara , Spain
Jolanta N. Latosinska , Poland
João Paulo Leal , Portugal
Woojin Lee, Kazakhstan
Yuan-Pern Lee , Taiwan
Matthias Lein , New Zealand
Huabing Li, China
Jinan Li , USA
Kokhwa Lim , Singapore
Teik-Cheng Lim , Singapore
Jianqiang Liu , China
Xi Liu , China
Xinyong Liu , China
Zhong-Wen Liu , China

Eulogio J. Llorent-Martínez , Spain
Pasquale Longo , Italy
Pablo Lorenzo-Luis , Spain
Zhang-Hui Lu, China
Devanand Luthria, USA
Konstantin V. Luzyanin , United Kingdom
Basavarajaiah S M, India
Mari Maeda-Yamamoto , Japan
Isabel Mafra , Portugal
Dimitris P. Makris , Greece
Pedro M. Mancini, Argentina
Marcelino Maneiro , Spain
Giuseppe F. Mangiatordi , Italy
Casimiro Mantell , Spain
Carlos A Martínez-Huitle , Brazil
José M. G. Martinho , Portugal
Andrea Mastinu , Italy
Cesar Mateo , Spain
Georgios Matthaiolampakis, USA
Mehrab Mehrvar, Canada
Saurabh Mehta , India
Oinam Romesh Meitei , USA
Saima Q. Memon , Pakistan
Morena Miciaccia, Italy
Maurice Millet , France
Angelo Minucci, Italy
Liviu Mitu , Romania
Hideto Miyabe , Japan
Ahmad Mohammad Alakraa , Egypt
Kaustubha Mohanty, India
Subrata Mondal , India
José Morillo, Spain
Giovanni Morrone , Italy
Ahmed Mourran, Germany
Nagaraju Mupparapu , USA
Markus Muschen, USA
Benjamin Mwashote , USA
Mallikarjuna N. Nadagouda , USA
Lutfun Nahar , United Kingdom
Kamala Kanta Nanda , Peru
Senthilkumar Nangan, Thailand
Mu. Naushad , Saudi Arabia
Gabriel Navarrete-Vazquez , Mexico
Jean-Marie Nedelec , France
Sridhar Goud Nerella , USA




Nagatoshi Nishiwaki , Japan
Tzortzis Nomikos , Greece
Beatriz P. P. Oliveira , Portugal
Leonardo Palmisano , Italy
Mohamed Afzal Pasha , India
Dario Pasini , Italy
Angela Patti , Italy
Massimiliano F. Peana , Italy
Andrea Penoni , Italy
Franc Perdih , Slovenia
Jose A. Pereira , Portugal
Pedro Avila Pérez , Mexico
Maria Grazia Perrone , Italy
Silvia Persichilli , Italy
Thijs A. Peters , Norway
Christophe Petit , France
Marinos Pitsikalis , Greece
Rita Rosa Plá, Argentina
Fabio Polticelli , Italy
Josefina Pons, Spain
V. Prakash Reddy , USA
Thathan Premkumar, Republic of Korea
Maciej Przybyłek , Poland
María Quesada-Moreno , Germany
Maurizio Quinto , Italy
Franck Rabilloud , France
C.R. Raj, India
Sanchayita Rajkhowa , India
Manzoor Rather , India
Enrico Ravera , Italy
Julia Revuelta , Spain
Muhammad Rizwan , Pakistan
Manfredi Rizzo , Italy
Maria P. Robalo , Portugal
Maria Roca , Spain
Nicolas Roche , France
Samuel Rokhum , India
Roberto Romeo , Italy
Antonio M. Romerosa-Nievas , Spain
Arpita Roy , India
Eloy S. Sanz P rez , Spain
Nagaraju Sakkani , USA
Diego Sampedro , Spain
Shengmin Sang , USA

Vikram Sarpe , USA
Adrian Saura-Sanmartin , Spain
St phanie Sayen, France
Ewa Schab-Balcerzak , Poland
Hartwig Schulz, Germany
Gulaim A. Seisenbaeva , Sweden
Serkan Selli , Turkey
Murat Senturk , Turkey
Beatrice Severino , Italy
Sunil Shah Shah , USA
Ashutosh Sharma , USA
Hideaki Shiota , Japan
Cl udia G. Silva , Portugal
Ajaya Kumar Singh , India
Vijay Siripuram, USA
Ponnurengam Malliappan Sivakumar ,
Japan
Tom s Sobrino , Spain
Raquel G. Soengas , Spain
Yujiang Song , China
Olivier Soppera, France
Radhey Srivastava , USA
Vivek Srivastava, India
Theocharis C. Stamataios , Greece
Athanasios Stavrakoudis , Greece
Darren Sun, Singapore
Arun Suneja , USA
Kamal Swami , USA
B.E. Kumara Swamy , India
Elad Tako , USA
Shoufeng Tang, China
Zhenwei Tang , China
Vijai Kumar Reddy Tangadanchu , USA
Franco Tassi, Italy
Alexander Tatarinov, Russia
Lorena Tavano, Italy
Tullia Tedeschi, Italy
Vinod Kumar Tiwari , India
Augusto C. Tome , Portugal
Fernanda Tonelli , Brazil
Naoki Toyooka , Japan
Andrea Trabocchi , Italy
Philippe Trens , France
Ekaterina Tsipis, Russia
Esteban P. Urriolabeitia , Spain

Toyonobu Usuki , Japan
Giuseppe Valacchi , Italy
Ganga Reddy Velma , USA
Marco Viccaro , Italy
Jaime Villaverde , Spain
Marc Visseaux , France
Balaga Viswanadham , India
Alessandro Volonterio , Italy
Zoran Vujcic , Serbia
Chun-Hua Wang , China
Leiming Wang , China
Carmen W ngler , Germany
Wieslaw Wiczowski , Poland
Bryan M. Wong , USA
Frank Wuest, Canada
Yang Xu, USA
Dharmendra Kumar Yadav , Republic of
Korea
Maria C. Yebra-Biurrun , Spain
Dr Nagesh G Yernale, India
Tomokazu Yoshimura , Japan
Maryam Yousaf, China
Sedat Yurdakal , Turkey
Shin-ichi Yusa , Japan
Claudio Zaccone , Italy
Ronen Zangi, Spain
John CG Zhao , USA
Zhen Zhao, China
Antonio Zizzi , Italy
Mire Zloh , United Kingdom
Grigoris Zoidis , Greece
Deniz  AH N , Turkey

Contents




Migration and Transformation of Heavy Metals in the Soil of the Water-Level Fluctuation Zone in the Three Gorges Reservoir under Simulated Nitrogen Deposition

Liuyi Zhang , Kun Fu, Fumo Yang , Yang Chen, Chuan Fu, Yimin Huang, Zhengjun Guo, and Tingzhen Li 

Research Article (10 pages), Article ID 6660661, Volume 2021 (2021)

Research Article

Migration and Transformation of Heavy Metals in the Soil of the Water-Level Fluctuation Zone in the Three Gorges Reservoir under Simulated Nitrogen Deposition

Liuyi Zhang ^{1,2}, Kun Fu,¹ Fumo Yang ^{1,2,3}, Yang Chen,^{1,2} Chuan Fu,¹ Yimin Huang,¹ Zhengjun Guo,¹ and Tingzhen Li ¹

¹Chongqing Key Laboratory of Water Environment Evolution and Pollution Control in Three Gorges Reservoir, Chongqing Three Gorges University, Wanzhou 404000, China

²CAS Key Laboratory of Reservoir Environment, Chongqing Institute of Green and Intelligent Technology, Chinese Academy of Sciences, Chongqing 400714, China

³National Engineering Research Center for Flue Gas Desulfurization, Department of Environmental Science and Engineering, Sichuan University, Chengdu 610065, China

Correspondence should be addressed to Fumo Yang; fmyang@scu.edu.cn and Tingzhen Li; lingtzh@163.com

Received 9 November 2020; Revised 18 January 2021; Accepted 31 January 2021; Published 19 February 2021

Academic Editor: Stanislav Frančišković-Bilinski

Copyright © 2021 Liuyi Zhang et al. This is an open access article distributed under the Creative Commons Attribution License, which permits unrestricted use, distribution, and reproduction in any medium, provided the original work is properly cited.

The accumulation of heavy metals (HMs) in the water-level fluctuation zone (WLFZ) of the Three Gorges Reservoir (TGR) area is potentially harmful to the water environment. In order to reveal whether nitrogen (N) deposition is a potential driving factor for the migration and transformation of HMs (Cd, Cr, Cu, Ni, and Pb), a simulated N deposition experiment was performed on the soil in the WLFZ of the TGR. The results showed that the accumulative release amounts of HMs increased with the increase of N deposition. It was found that the Elovich equation, double-constant equation, and parabolic diffusion equation could well describe the release process of Cu, Cd, Cr, and Ni, while the double-constant equation, parabolic diffusion equation, and first-order equation could be applicable for Pb. The exchangeable fractions of HMs increased to varying degrees after the N deposition treatment, wherein Ni was most significant, indicating that N deposition could increase the ecological risk of HM pollution in the TGR area. The results provide insight into the major factors affecting the release of different HMs under N deposition in this vulnerable region ecologically.

1. Introduction

The Three Gorges Reservoir (TGR) area is located in the middle and upper reaches of the Yangtze River, south-western China. The TGR stores water from October to April and discharges water from May to September, resulting in the water-level fluctuation between 135 m and 145 m, and the formation of a water-level fluctuation zone (WLFZ) with an area of 348.9 km². Affected by the periodic flooding, the ecological environment of the WLFZ is fragile, and the related environmental problems, e.g., accumulation of heavy metals (HMs), have raised the attention [1, 2]. Since the initial impoundment of the TGR, HMs in the WLFZ soil

have shown an upward trend because of the external inputs from agricultural activities and domestic wastes [3]. Of note is that the cumulative HMs, in turn, can become the potential source of pollution and threaten the safety of the water environment.

Factors affecting the activity and mobility of HMs in the soil of WLFZ in the TGR are implicated in two aspects. Firstly, the local agricultural activities, such as plowing and fertilization in WLFZ during the period of exposure, can accelerate the migration of HMs from WLFZ to the water body of the TGR [4, 5]. However, with the government's prohibition of agricultural activities on WLFZ, this impact has been minimal. Secondly, the changes of physical,

chemical, and biological properties of soil under periodic recession (oxidation) and inundation (reduction) can cause the transformation and migration of HMs. Related research studies have made great progress [6].

Agricultural activities and periodic fading and flooding conditions are currently the two most concentrated researches on the migration and transformation of HMs in the WFLZ of the TGR area. To the best of our knowledge, however, the impact of precipitation on migration and transformation is rarely reported. Atmospheric precipitation, another important factor affecting the environmental behaviors of HMs in soil, involves not only physical migration but also involves chemical transformation depending on the chemical compositions of precipitation. Nitrogen (N) is the main chemical component in precipitation, mainly in the inorganic form (NO_3^- -N and NH_4^+ -N) and also includes a small amount of organic N. In recent years, not only the N flux of wet deposition has a great increase, but the N forms in a wet deposition have also been changed [7]. In this case, the response of the ecological environment to N deposition is particularly worthy of attention.

In the TGR area, a relatively higher level of N flux deposition ($26.81 \pm 13.83 \text{ kg N ha}^{-1} \text{ yr}^{-1}$) is threatening the aquatic and forest ecosystems, even some farmland ecosystems [8, 9]. Excessive N deposition can cause soil acidification and further increase the solubility of potentially toxic metals in soil [10]. The exposure period of the WFLZ soil coincides with the rainy season (May to September), in which wet deposition N accounts for about 70% [9, 11]. Therefore, we collected undisturbed WFLZ soil columns and performed a simulated N deposition experiment to study the mobility characteristics of typical HMs, aiming to explore the relationship between N deposition and the migration and transformation of HMs in the WFLZ soil. This information has implications for better understanding the migration and transformation of HMs in the TGR area.

2. Materials and Methods

2.1. Sample Collection. A gentle WFLZ was selected at 154 m of water-level elevation in the Tanshao village, Wanzhou District (Figure 1); 12 undisturbed soil samples were collected with clean PVC pipes (15 cm in diameter and 20 cm in height). After collection, we covered both ends of the soil pillar samples with plastic wrap and brought them back to the laboratory for subsequent N addition experiment. The physicochemical properties of soil in WFLZ and concentrations of HMs are shown in Table 1. The single factor index method was applied to assess the pollution degree of HMs. The pollution index (P_i) for each HM was expressed by the ratio of the measured concentration (C_i , mg/kg) to the standard concentration (C_{is} , mg/kg) [12]. In this study, the background value of HMs in the WFLZ was used as the standard value [13]. Based on the results of single factor index method [12], Cd belonged to a high pollution degree ($P_i > 3$), while Cr, Cu, Ni, Pb, and Zn belonged to clean level ($P_i < 1$) in the original WFLZ soil in this study (Table 1).

2.2. Simulation of N Deposition. According to the N deposition flux ($20.69 \text{ kgN/ha}\cdot\text{yr}$) and the average annual rainfall ($\sim 1200 \text{ mm}$) in the TGR area [8], four N flux groups, including N-free group (N_0 , $0 \text{ kgN/ha}\cdot\text{yr}$), low N group (N_{20} , $20 \text{ kgN/ha}\cdot\text{yr}$), middle N group (N_{40} , $40 \text{ kgN/ha}\cdot\text{yr}$), and high N group (N_{60} , $60 \text{ kgN/ha}\cdot\text{yr}$), were set, and each group was performed in triplicate. N_0 , N_{20} , N_{40} , and N_{60} were about 0, 1, 2, and 3 times, respectively, of the actual N deposition fluxes in the TGR area. NH_4NO_3 was the only N source in this research, and the pH of each leaching solution was adjusted to 5.5, which was consistent with the local rainwater [11].

Siphon drip irrigation bags with adjustable flow rates were used to hold the leaching solution, and the flow rate was set to 0.8 mL/min to prevent water from accumulating in the soil column. Before leaching, two $0.45 \mu\text{m}$ microporous membranes at both ends of the soil column were fixed. The leaching volume was 0.5 L each day, and this process of leaching was continued for 40 days. 20 L of the total leaching volume (about 1162.6 mm rainfall amount) was consistent with the local multiyear average rainfall amount (about 1150 mm). The schematic diagram of the simulated N addition device was shown in Figure 2. After finishing the daily leaching, the volume of each leachate was recorded firstly and then filtered through $0.45 \mu\text{m}$ filter membrane and stored at 4°C for testing. Soil samples before and after eluviation were air-dried at room temperature, and then the plant roots and residues were removed. Hereafter, the soil samples were homogenized and grounded to pass through a 2-mesh sieve for determining the physicochemical properties and the metal fractions.

2.3. Sample Analysis. Soil pH (H_2O) was determined in 1 : 2.5 (w/v) soil water suspension using PHS-3C pH-meter (Shanghai Leici Instrument Co., Ltd, China). Organic matter was determined by a modified Walkley-Black method, and the detailed processes have been described elsewhere [14]. NH_4^+ and NO_3^- in the samples were analyzed by an ion chromatograph (Dionex-900, Dionex, USA) with detection limits of 0.005 mg/L and 0.031 mg/L , respectively.

In order to determine the mobility and activity of HMs, the exchangeable fraction of typical HMs (Cd, Cr, Cu, Ni, and Pb) was extracted by the classical method [15]. In brief, 1 g of dried sample was extracted with 8 mL MgCl_2 ($\text{pH} = 7.0$) and continually shaken for 1 hour at 25°C , the extract was centrifuged at 4000 rpm , and the supernatant was made to volume in 25 mL volumetric flask. The residual soil was digested with a mixed acid (6 mL of HNO_3 , 2 mL of HCl , and 2 mL of HF) by microwave digestion instrument (Mars5, CEM, USA). HMs were determined by inductively coupled plasma optical emission spectrometry (Optima 7000, PerkinElmer, USA). The detection limits were 0.006 , 0.03 , 0.008 , 0.33 , and 0.035 g/L , respectively. The recovery rates of samples were between 95% and 120%.

2.4. Statistical Processing of Data. In this study, the double-constant equation (1), Elovich equation (2), first-order equation (3), and parabolic diffusion equation (4) were used

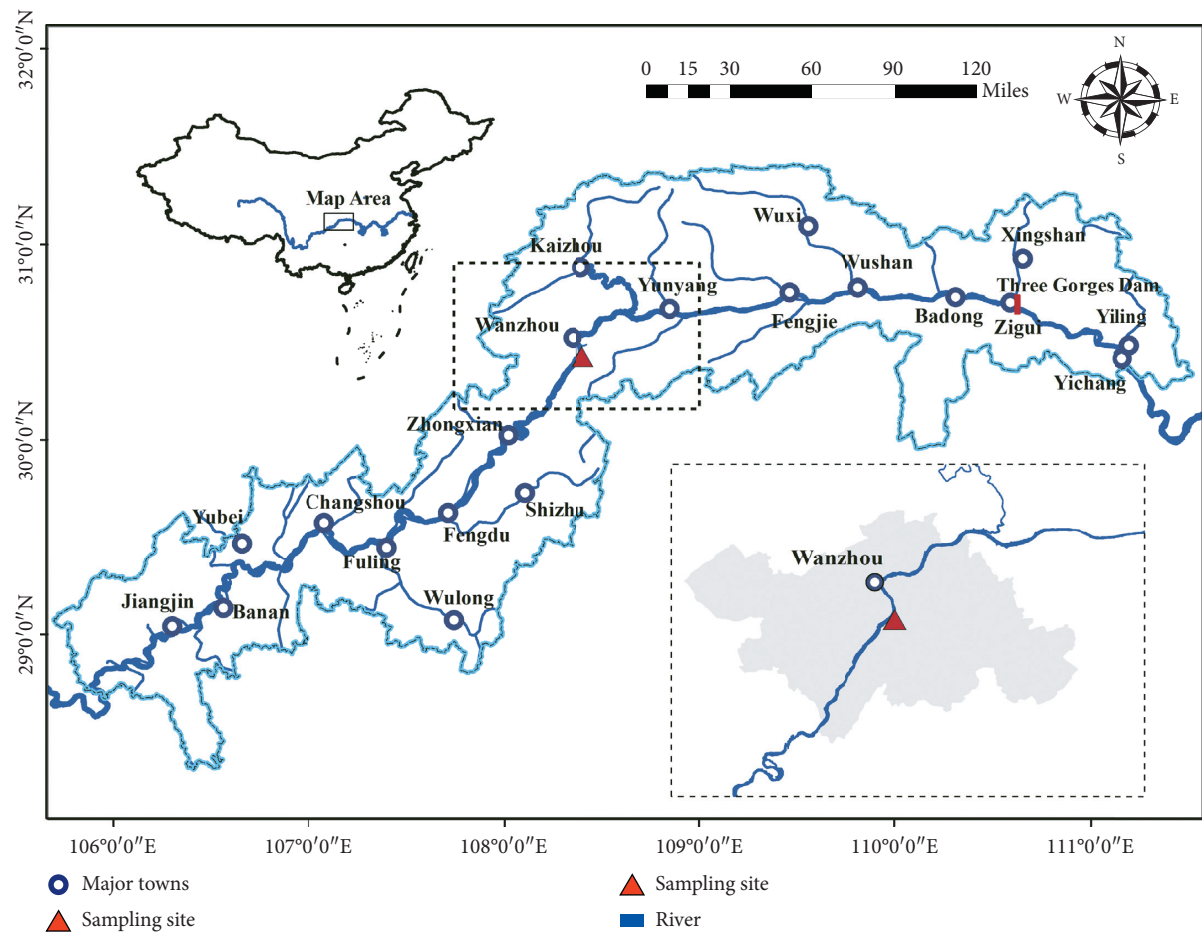


FIGURE 1: Location of the sampling site.

TABLE 1: Physicochemical properties of the original WFLZ soil in the TGR area.

Soil indexes	Content	Background values of WFLZ in the TGR ^a	Pollution degree ^b
pH	8.16 ± 0.13	7.84	n.d
OM (g/kg)	13.92 ± 0.47	n.d	n.d
Bulk density (g/cm ³)	1.4 ± 0.14	n.d	n.d
NO ₃ ⁻ -N (mg/kg)	2.13 ± 0.007	n.d	n.d
NH ₄ ⁺ -N (mg/kg)	179.49 ± 6.47	n.d	n.d
Al (%)	3.98 ± 0.38	n.d	n.d
Fe (%)	4.88 ± 0.49	n.d	n.d
Mn (mg/kg)	1018.66 ± 149.05	n.d	n.d
Cd (mg/kg)	2.63 ± 0.67	0.321	High
Cr (mg/kg)	76.82 ± 5.89	55.5	Clean
Cu (mg/kg)	37.17 ± 5.13	37	Clean
Ni (mg/kg)	48.46 ± 0.95	29.5	Clean
Pb (mg/kg)	65.80 ± 7.64	29.3	Clean
Zn (mg/kg)	166.82 ± 21.89	72.7	Clean

^aBackground values of WFLZ in the TGR [13]. ^bEvaluation by single factor index method [12]. n.d. means no data.

to describe the release kinetics of HMs under N deposition [16].

$$\ln S = a \ln t + b, \tag{1}$$

$$S = a \ln t + b, \tag{2}$$

$$\ln \left(\frac{S}{S_m} \right) = at + b, \tag{3}$$

$$\frac{S}{S_m} = at^{1/2} + b, \tag{4}$$

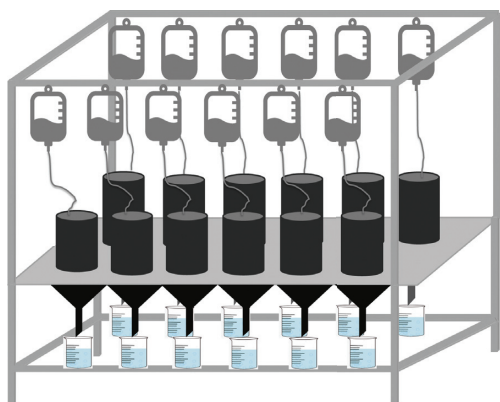


FIGURE 2: Leaching device of simulating N deposition.

where S ($\mu\text{g/kg}$) is the release amount of metals at a certain time, S_m ($\mu\text{g/kg}$) is the maximum release amount, t (d) is the leaching time, a and b are the constants with different meanings for each model.

One-way analysis of variance (ANOVA) was used to test for differences between groups of N deposition if the data conform to the normal distribution. Otherwise, Kruskal-Wallis rank sum test was applied to test the differences. In addition, Person's correlation coefficient was used to describe the relationships between variables. These analyses were performed using IBM SPSS version 22.0 statistical software.

3. Results and Discussion

3.1. Cumulative Release Amount. The cumulative release amounts of HMs were different under various treatments of N deposition (Table 2). Both Cr and Cu were leached out more than $30 \mu\text{g}$, and the amounts under N_{60} treatment were significantly higher ($p < 0.05$) than those under N_0 , N_{20} , and N_{40} treatments. In contrast, the release amounts of Ni and Cd were lower than $10 \mu\text{g}$, and there were no significant differences ($p > 0.05$) between each N deposition treatment. In addition, the amount of leached-out Pb showed a significant difference between each N treatment. The results indicated that Pb was the most sensitive to the N deposition, and even a low N deposition load ($20 \text{ kgN}/(\text{ha yr})$) could stimulate the release of Pb from WFLZ soil. This could be ascribed to the relatively lower binding energy of Pb with Fe/Al hydro(oxide) in the WFLZ soil, which was more susceptible to the destruction of N deposition [17, 18]. However, a high N deposition load ($60 \text{ kgN}/(\text{ha yr})$) was required to promote the release of Cr and Cu significantly. Besides, there was no significant influence on the release of Cd and Ni under the treatments of N deposition in this study.

3.2. Release Rate. Under the simulated precipitation leaching, HMs presented three different release stages except that Cr showed two stages (Figure 3). Every release stage of HMs showed a good linear relationship ($r^2 > 0.85$), and the slopes of the linear equations can be used to represent the release rate of HMs at each stage. The linear equations

TABLE 2: Cumulative release amounts of HMs in the soil of WFLZ in the TGR area (unit: μg).

Treatment	Cr	Cu	Cd	Ni	Pb
N_0	32.44a	30.45a	1.61a	7.29a	6.76a
N_{20}	34.21a	30.83a	1.69a	7.98a	14.27b
N_{40}	35.08a	32.18a	1.67a	8.52a	22.74c
N_{60}	38.82b	36.08b	1.87a	7.90a	31.15d

Note. The same letters mean no significant difference ($p > 0.05$) and different letters mean significant difference ($p < 0.05$) tested by one-way ANOVA.

and coefficients (r^2) were shown in Table 3. The release rates of Cr, Cu and Cd exhibited a similar variation trend, showing the fastest release rate in the first stage, and gradually decreasing in the following stages. This may be related to the contents of water-soluble ions in the soil. In the beginning stage, the metal ions in the soil water were quickly released with the wet deposition. As the leaching continued in the second stage, the adsorbed HMs were gradually leached out. In the third stage, the release rate became slower as the active ions of HMs decreased, and this stage may involve chemical transformation and desorption. Since Cr usually presents in the soil in the form of negative valent acid radical ($\text{Cr}_2\text{O}_7^{2-}$ and CrO_4^{2-}), which were hardly adsorbed by soil colloid and easily mobilized in soil [19], only a two-stage leaching process was exhibited. The cumulative release rate of Ni increased instead after 32 days (the third stage), probably caused by some chemically bound forms leaching out. For Pb, the cumulative release curve fluctuated greatly, and there existed large differences in its release amount with different N deposition levels, pointing to more intricate physicochemical processes of soil Pb due to N deposition.

3.3. Kinetics of Cumulative Release. The first-order kinetic equation, double-constant rate equation, parabolic equation, and modified Elovich equation are the common mathematical models to describe the characteristics of dynamics of soil HMs [20, 21]. The first-order kinetic equation is good at describing the simpler surface process of the diffusion mechanism [22]. The double-constant rate equation (also known as Freundlich's correction) is an empirical formula, which is suitable for more complex kinetic reaction processes and can better describe the uneven energy distribution process and the different affinity of adsorption sites to HMs on the surface of soil particles [16]. The parabolic equation is suitable to describe the process controlled by multiple diffusers [23]. The Elovich equation is also an empirical formula, which describes a process that includes a series of reaction mechanisms, such as the diffusion of solutes at the solution phase or interface, surface activation, and deactivation [24]. The equation is suitable for the reactions with large changes in activation energy processes (such as those on sediments and soils), which are less suitable for processes with a single surface diffusion mechanism [25]. The above four equations were used to fit the leaching data obtained in this research. The fitting results are shown in Table 3.

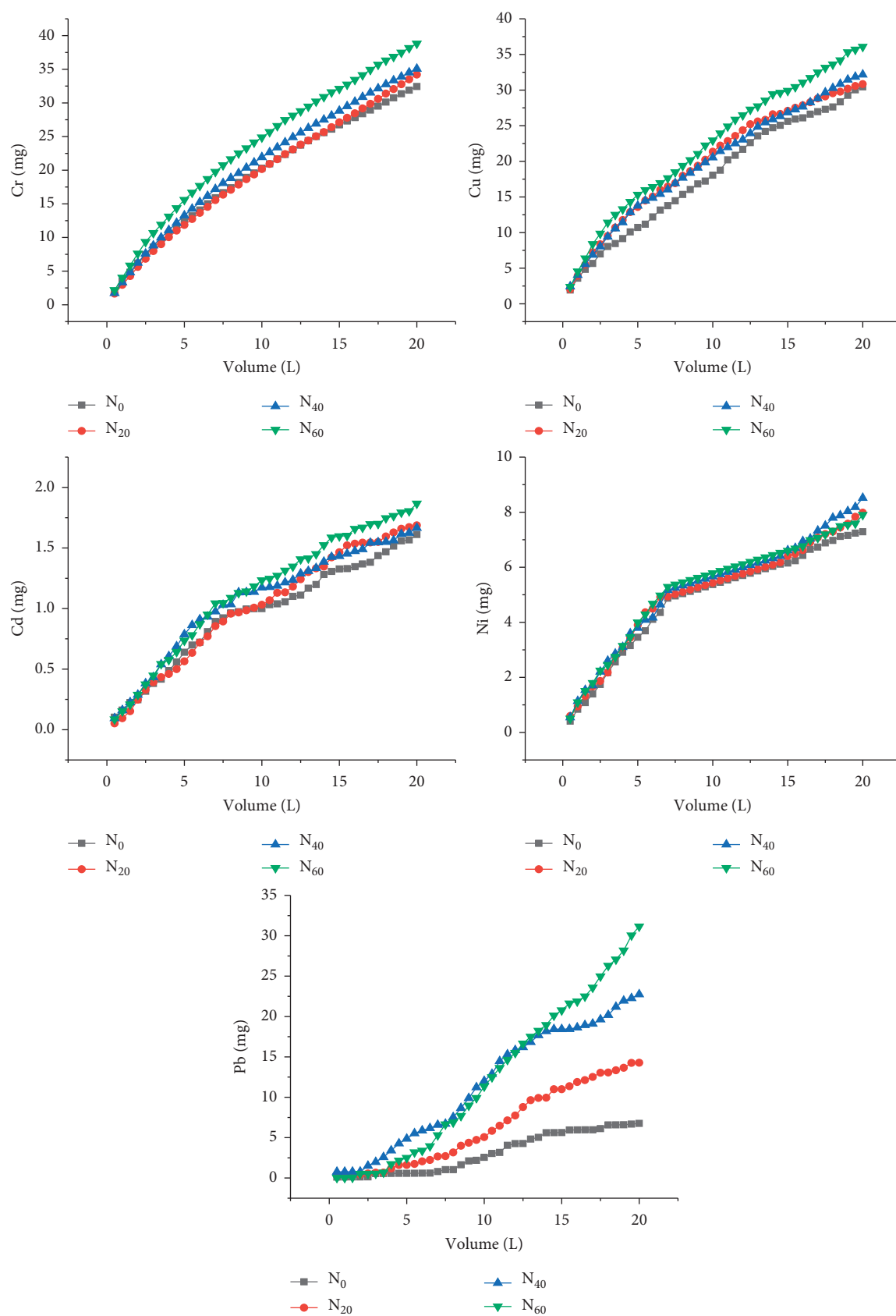


FIGURE 3: Cumulative release amounts of HMs in the soil of the WFLZ in the TGR area.

TABLE 3: Fitting functions of cumulative release amounts and the release rates of HMs.

N deposition	Release process	Fitting equation	Correlation coefficient (r^2)	Release rate ($\mu\text{g/d}$)
<i>Cr</i>				
N_0	First stage	$y = 1.14x + 1.38$	0.992	1.14
	Second stage	$y = 0.65x + 7.03$	0.996	0.65
N_{20}	First stage	$y = 1.14x + 0.84$	0.995	1.14
	Second stage	$y = 0.72x + 5.49$	0.999	0.72
N_{40}	First stage	$y = 1.27x + 0.92$	0.995	1.27
	Second stage	$y = 0.71x + 7.50$	0.996	0.71
N_{60}	First stage	$y = 1.48x + 1.34$	0.991	1.48
	Second stage	$y = 0.76x + 9.63$	0.995	0.76
<i>Cu</i>				
N_0	First stage	$y = 1.09x + 1.28$	0.982	1.09
	Second stage	$y = 0.78x + 2.86$	0.997	0.78
	Third stage	$y = 0.46x + 11.63$	0.989	0.46
N_{20}	First stage	$y = 1.43x + 1.04$	0.989	1.43
	Second stage	$y = 0.78x + 5.70$	0.998	0.78
	Third stage	$y = 0.38x + 15.66$	0.998	0.38
N_{40}	First stage	$y = 1.34x + 1.33$	0.997	1.34
	Second stage	$y = 0.70x + 6.39$	0.997	0.70
	Third stage	$y = 0.54x + 10.62$	0.997	0.54
N_{60}	First stage	$y = 1.70x + 1.13$	0.991	1.70
	Second stage	$y = 0.82x + 6.57$	0.995	0.82
	Third stage	$y = 0.60x + 12.23$	0.996	0.60
<i>Cd</i>				
N_0	First stage	$y = 0.06x + 0.03$	0.995	0.06
	Second stage	$y = 0.03x + 0.51$	0.927	0.03
	Third stage	$y = 0.03x + 0.28$	0.982	0.03
N_{20}	First stage	$y = 0.06x - 0.005$	0.991	0.06
	Second stage	$y = 0.04x + 0.31$	0.980	0.04
	Third stage	$y = 0.02x + 0.88$	0.933	0.02
N_{40}	First stage	$y = 0.07x + 0.02$	0.991	0.07
	Second stage	$y = 0.03x + 0.64$	0.968	0.03
	Third stage	$y = 0.02x + 0.76$	0.961	0.02
N_{60}	First stage	$y = 0.07x + 0.005$	0.998	0.07
	Second stage	$y = 0.04x + 0.49$	0.989	0.04
	Third stage	$y = 0.03x + 0.81$	0.973	0.03
<i>Ni</i>				
N_0	First stage	$y = 0.33x + 0.12$	0.997	0.33
	Second stage	$y = 0.08x + 3.72$	0.997	0.08
	Third stage	$y = 0.09x + 3.55$	0.975	0.09
N_{20}	First stage	$y = 0.36x + 0.22$	0.993	0.36
	Second stage	$y = 0.09x + 3.63$	0.990	0.09
	Third stage	$y = 0.15x + 1.94$	0.986	0.15
N_{40}	First stage	$y = 0.33x + 0.47$	0.995	0.33
	Second stage	$y = 0.09x + 3.84$	0.985	0.09
	Third stage	$y = 0.19x + 0.70$	0.982	0.19
N_{60}	First stage	$y = 0.36x + 0.33$	0.998	0.36
	Second stage	$y = 0.08x + 4.14$	0.999	0.08
	Third stage	$y = 0.12x + 2.94$	0.965	0.12
<i>Pb</i>				
N_0	First stage	$y = 0.06x + 0.01$	0.850	0.06
	Second stage	$y = 0.36x - 4.53$	0.984	0.36
	Third stage	$y = 0.11x + 2.54$	0.932	0.11
N_{20}	First stage	$y = 0.19x - 0.19$	0.937	0.19
	Second stage	$y = 0.62x - 6.97$	0.985	0.62
	Third stage	$y = 0.34x + 0.84$	0.979	0.34
N_{40}	First stage	$y = 0.51x - 0.59$	0.993	0.51
	Second stage	$y = 0.92x - 6.62$	0.979	0.92
	Third stage	$y = 0.40x + 6.29$	0.900	0.40
N_{60}	First stage	$y = 0.44x - 1.41$	0.895	0.44
	Second stage	$y = 1.07x - 10.21$	0.996	1.07
	Third stage	$y = 1.00x - 9.26$	0.977	1.00

TABLE 4: Fitting parameters of each kinetic model for HMs in the WFLZ soil in the TGR area under N deposition.

HMs	N load	Elovich equation $S = a \ln t + b$			Double-constant equation $\ln S = a \ln t + b$			First-order equation $\ln(S/S_m) = at + b$			Parabolic diffusion equation $S/S_m = at^{1/2} + b$		
		A	B	R^2	a	b	R^2	a	b	R^2	a	b	R^2
Cr	N ₀	22.71	-15.98	0.912	0.7375	1.6570	0.998	0.0495	-0.2814	0.805	0.7342	-0.7290	0.996
	N ₂₀	24.03	-19.40	0.896	0.7999	1.4668	0.998	0.0537	-0.3862	0.806	0.7824	-0.9239	0.992
	N ₄₀	24.98	-18.65	0.915	0.7807	1.5989	0.995	0.0517	-0.2670	0.783	0.8069	-0.8541	0.997
	N ₆₀	27.22	-18.29	0.926	0.7433	1.8387	0.993	0.0490	-0.0745	0.774	0.8746	-0.8052	0.999
Cu	N ₀	21.41	-15.98	0.888	0.7342	1.5831	0.997	0.0503	-3.5867	0.837	0.0283	-0.0308	0.987
	N ₂₀	21.91	-12.55	0.937	0.6957	1.8161	0.990	0.0457	-3.3657	0.765	0.0283	-0.0208	0.997
	N ₄₀	22.03	-13.22	0.920	0.6825	1.8470	0.997	0.0458	-3.3738	0.805	0.0288	-0.0234	0.997
	N ₆₀	24.51	-14.23	0.919	0.6826	1.9633	0.992	0.0455	-3.2502	0.788	0.0320	-0.0249	0.995
Cd	N ₀	1.1235	-0.7942	0.920	0.7580	-1.4149	0.988	0.0504	-6.0825	0.781	0.0023	-0.0022	0.989
	N ₂₀	1.2880	-1.1353	0.909	0.9208	-1.8707	0.985	0.0599	-6.2842	0.745	0.0026	-0.0033	0.993
	N ₄₀	1.1909	-0.7221	0.954	0.7594	-1.3068	0.973	0.0485	-5.9317	0.710	0.0024	-0.0017	0.988
	N ₆₀	1.3679	-1.0362	0.932	0.8253	-1.4479	0.986	0.0536	-5.9971	0.745	0.0028	-0.0028	0.995
Ni	N ₀	5.191	-2.730	0.961	0.7325	0.2866	0.965	0.0461	-3.7091	0.685	0.0196	-0.0113	0.977
	N ₂₀	5.257	-2.398	0.950	0.6747	0.5061	0.969	0.0432	-3.5899	0.713	0.0199	-0.0095	0.975
	N ₄₀	5.476	-2.533	0.945	0.6677	0.5663	0.976	0.0430	-3.5448	0.727	0.0209	-0.0107	0.983
	N ₆₀	5.289	-2.055	0.966	0.6673	0.5661	0.961	0.0419	-3.5221	0.678	0.0199	-0.0064	0.971
Pb	N ₀	5.730	-8.348	0.698	1.4801	-2.6781	0.915	0.1096	-5.4861	0.898	0.0367	-0.0859	0.873
	N ₂₀	11.39	-16.09	0.717	1.3214	-1.4157	0.924	0.0986	-4.4358	0.921	0.0730	-0.1654	0.893
	N ₄₀	18.21	-22.30	0.817	1.1846	-0.3050	0.955	0.0828	-3.3801	0.837	0.1128	-0.2150	0.952
	N ₆₀	23.20	-34.11	0.729	2.1463	-3.3404	0.975	0.1416	-4.9676	0.760	0.1482	-0.3483	0.904

Note. Correlation coefficients (R^2) higher than 0.9 are in bold.

Based on the correlation coefficients (R^2) fitted by each equation (Table 4), it was found that the double-constant equation and parabolic equation can better describe the kinetic process of leaching of HMs in the WFLZ soil by simulated N deposition. At the same time, Cr, Cu, Cd, and Ni had a relatively high correlation coefficient of the Elovich equation, while Pb had a relatively higher correlation coefficient of the first-order equation. The results indicated that being controlled by the intricate reaction rate and the multidiffusion factors were the common kinetics' features of these HMs. In addition, the relatively good fitting of the Elovich equation for Cr, Cu, Cd, and Ni suggested that the mechanism of leaching and release of these elements in WFLZ soil was also influenced by the changes in activation energy, rather than a single surface diffusion process, while the release of Pb was also affected by single surface diffusion.

3.4. Activation of HMs. The exchangeable fraction of HMs was relatively low, but its mobility and activity were the highest in HM forms. In this study, exchangeable fractions of Cd, Cu, Ni, Pb, and Cr were 0.13, 0.20, 0.47, 0.60, and 0.81 mg/kg, accounting for 4.90%, 0.54%, 0.96%, 0.90%, and 1.05% of the total mass contents, respectively. Figure 4 presents the changes of an exchangeable fraction of HMs before (original) and after leaching (N₀, N₂₀, N₄₀, and N₆₀). It can be seen that the N deposition stimulated the increase of HMs' exchangeable fraction. For Cr, Cu, and Pb, the exchangeable fractions between each treatment of N deposition had no significant change ($p > 0.05$). For Cd, the exchangeable fractions after leaching (N₀, N₂₀, N₄₀, and N₆₀) were significantly higher than the original one, but there were no significant differences between the N-containing

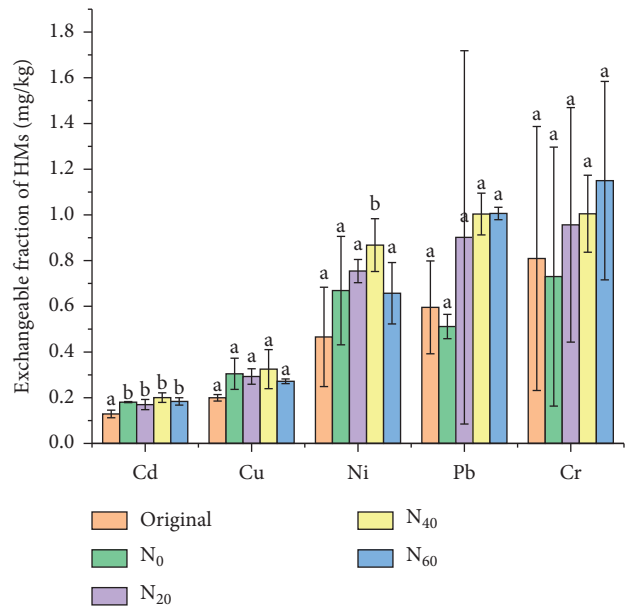


FIGURE 4: Changes of exchangeable fractions of HMs before (original) and after leaching (N₀, N₂₀, N₄₀, and N₆₀).

group (N₂₀, N₄₀, and N₆₀) and the N-free group (N₀). This may be affected by the pH (5.5) rather than the N of the leaching solution. For Ni, the exchangeable fraction after leaching by N₄₀ was significantly higher than other groups. It was consistent with the aforementioned release amount of Ni. The results showed that N deposition was more conducive to promoting the activation of Ni compared with Cd, Cr, Cu, and Pb.

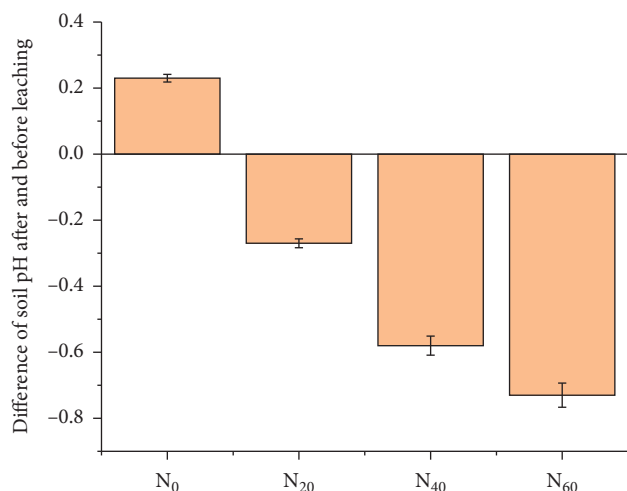


FIGURE 5: Changes of soil pH after and before leaching at different N deposition levels.

4. Discussion

The mechanism of N deposition-induced acidification of soil is different from acid deposition. Acidic deposition brings H^+ directly into the soil to activate trace metals, and the H^+ can displace the exchangeable fractions from their binding sites [26, 27]. Different HMs have different sensitivity to acid deposition. For purple soil in the Sichuan Basin, the transformability and mobility of Cu and Zn by acid deposition were higher than that of Pb and Cd [28]. However, the activation and migration of HMs induced by N deposition have latent characteristics. First, NH_4^+ displaces the base cations, resulting in the base cations being lost with NO_3^- and reducing the buffering capacity for soil acidity [29]. Additionally, plant-induced assimilation ($NH_4^+ + ROH \rightarrow RNH_2 + H_2O + H^+$) and soil-induced nitrification would release H^+ to cause soil acidification [30], and the H^+ further promotes HMs' transformation and migration.

In this study, although this decrease was not significant ($p > 0.05$), the pH of WLFZ soil decreased with increasing N deposition (Figure 5), showing that N deposition has a potential acidification effect. Since this study did not involve plant ecosystems, this insignificant acidification may be attributed to the nitrification of soil NH_4^+ because NH_4NO_3 can promote the growth of soil nitrifying bacteria and accelerate the rate of soil nitrification, thereby accelerating soil acidification [31]. In addition, the leaching amounts of base cations (K^+ , Na^+ , Ca^{2+} , and Mg^{2+}) were increased as increasing N deposition (Figure 6), and the concentrations of base cations were all positively correlated with NO_3^- in leachate (r^2 ranged from 0.16–0.92, $p < 0.01$). Therefore, it was the NO_3^- that carried the base cations to loss with wet deposition. With the loss of base cations, the acid buffering of soil decreased, and toxic HMs began to active and migrate, resulting in ecological harm.

The WLFZ is a land-water interlaced zone. Thus there exist frequent material and energy exchanges between the WLFZ soil and the water body in the TGR area [32]. The high background content and the accumulating HMs in

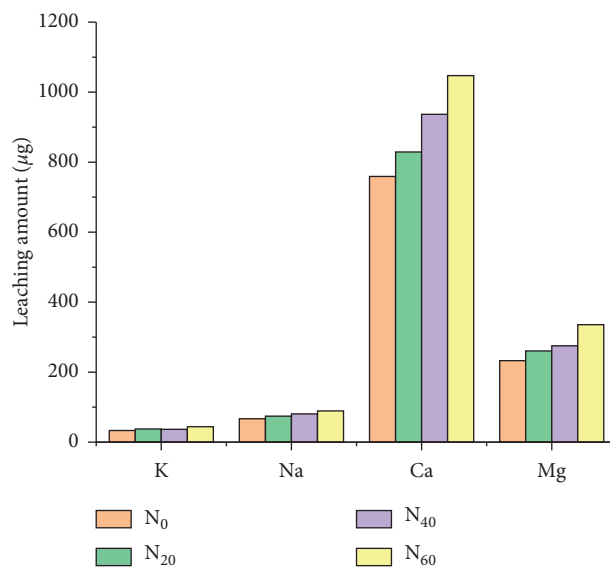


FIGURE 6: Leaching amounts of base cations under N deposition.

WLFZ soil as a result of external inputs (e.g., sewage discharge, agricultural nonpoint sources) have become the potential pollution sources of the TGR [1, 33, 34]. Under the influence of external environmental disturbance, these HMs will be activated and migrated, causing harm to the ecosystem. This study showed that N deposition was a non-negligible factor driving the transformation and migration of HMs. A moderate level of N deposition (40 kgN/(ha·yr)) could cause significant activation of Ni and cause migration of Cd, Cu, Pb, and Cr with wet deposition. According to our previous study, the N flux of wet deposition in the entire TGR area ranged from 12.17 to 51.93 kgN/(ha·yr), and it could exceed 40 kgN/(ha·yr) in the upstream area [8]. Therefore, the influence of N deposition on the migration and transformation of HMs in the soil of the WLFZ is worthy of in-depth exploration.

5. Conclusions

The effect of N deposition on the migration and transformation of HMs in the fluctuation zone of the TGR was investigated in this study. As the N deposition increased, the amounts of leached-out HMs increased. The cumulative release amounts of Cr and Cu were much higher than those of Pb, Ni, and Cd, whereas that of Pb showed significant differences between N deposition groups. Three-stage dissolution for Cu and Cd was observed. Their dissolution rates were gradually lower, and only physical elution was involved. In contrast, the dissolution rate of Ni increased at the third stage, likely caused by the activation effects. In comparison, Cr only experienced two stages of rapid and slow dissolution. The double-constant equation and the parabolic diffusion equation could well describe the leaching process of HMs, indicating that the release process of the HMs was a diffusion kinetic process with uneven energy distribution and controlled by multiple diffusion factors. After the N deposition treatment, the exchangeable fractions of HMs

increased to varying degrees, of which Ni was most significant, indicating that N deposition would enhance the ecological risk of HM pollution in the TGR area, a unique region with a vulnerable ecology environment.

Data Availability

The data used to support the findings of this study are included within the article.

Conflicts of Interest

The authors declare that there are no conflicts of interest regarding the publication of this paper.

Acknowledgments

This work was supported by the National Natural Science Foundation of China (No. 31670467), the Science and Technology Commission of Chongqing project (No. cstc2018jcyjAX0236), the West Action Plan of the Chinese Academy of Science (No. KZCX2-XB3-14), and the open fund of CAS Key Laboratory of Reservoir Aquatic Environment.

References

- [1] C. Ye, S. Li, Y. Zhang, and Q. Zhang, "Assessing soil heavy metal pollution in the water-level-fluctuation zone of the Three Gorges Reservoir, China," *Journal of Hazardous Materials*, vol. 191, no. 1-3, pp. 366–372, 2011.
- [2] X. Zhao, B. Gao, D. Xu, L. Gao, and S. Yin, "Heavy metal pollution in sediments of the largest reservoir (Three Gorges Reservoir) in China: a review," *Environmental Science and Pollution Research*, vol. 24, no. 26, pp. 20844–20858, 2017.
- [3] S. Pei, Z. Jian, Q. Guo et al., "Temporal and spatial variation and risk assessment of soil heavy metal concentrations for water-level-fluctuating zones of the Three Gorges Reservoir," *Journal of Soils and Sediments*, vol. 18, no. 9, pp. 2924–2934, 2018.
- [4] Q. Y. Chen, S. Sun, D. L. Yin, L. M. Wang, C. Zhang, and D. Y. Wang, "Effects of agricultural activities on soil mercury changes in the water-level-fluctuating zone of the three Gorges reservoir," *Environ Sci*, vol. 39, pp. 2456–2463, 2018, in Chinese.
- [5] F. Ye, M. H. Ma, S. J. Wu et al., "Soil properties and distribution in the riparian zone: the effects of fluctuations in water and anthropogenic disturbances," *European Journal of Soil Science*, vol. 70, no. 3, pp. 664–673, 2019.
- [6] Y. Wang, P. Huang, F. Ye et al., "Nitrite-dependent anaerobic methane oxidizing bacteria along the water level fluctuation zone of the Three Gorges Reservoir," *Applied Microbiology and Biotechnology*, vol. 100, no. 4, pp. 1977–1986, 2016.
- [7] G. Yu, Y. Jia, N. He et al., "Stabilization of atmospheric nitrogen deposition in China over the past decade," *Nature Geoscience*, vol. 12, no. 6, pp. 424–429, 2019.
- [8] Q. Leng, J. Cui, F. Zhou et al., "Wet-only deposition of atmospheric inorganic nitrogen and associated isotopic characteristics in a typical mountain area, southwestern China," *Science of the Total Environment*, vol. 616-617, pp. 55–63, 2018.
- [9] L. Zhang, M. Tian, C. Peng et al., "Nitrogen wet deposition in the Three Gorges Reservoir area: characteristics, fluxes, and contributions to the aquatic environment," *Science of the Total Environment*, vol. 738, Article ID 140309, 2020.
- [10] C. J. Stevens, N. B. Dise, and D. J. Gowing, "Regional trends in soil acidification and exchangeable metal concentrations in relation to acid deposition rates," *Environmental Pollution*, vol. 157, no. 1, pp. 313–319, 2009.
- [11] L. Zhang, B. Qiao, H. Wang et al., "Chemical characteristics of precipitation in a typical urban site of the hinterland in three Gorges reservoir, China," *Journal of Chemistry*, vol. 2018, Article ID 2914313, 10 pages, 2018.
- [12] N. Yan, W. Liu, H. Xie et al., "Distribution and assessment of heavy metals in the surface sediment of Yellow River, China," *Journal of Environmental Sciences*, vol. 39, pp. 45–51, 2016.
- [13] Q. Li, Q. Zhang, H. L. Liu, and X. Zhou, "The investigation on the heavy metal pollution of the soil in inundated area in the ChongQing Reservoir," *Studies on Trace Element Health*, vol. 24, pp. 34–36, 2007, in Chinese.
- [14] L. Chen, D. F. Flynn, X. Jing, P. Kuhn, T. Scholten, and J. S. He, "A comparison of two methods for quantifying soil organic carbon of alpine grasslands on the Tibetan Plateau," *PLoS One*, vol. 10, p. e0126372, 2015.
- [15] A. Tessler, P. G. C. Campbell, and M. Bisson, "Sequential extraction procedure for the speciation of particulate trace metals," *Analytical Chemistry*, vol. 51, pp. 844–851, 1979.
- [16] Y. Yang, L. Liang, and D. Wang, "Effect of dissolved organic matter on adsorption and desorption of mercury by soils," *Journal of Environmental Sciences*, vol. 20, no. 9, pp. 1097–1102, 2008.
- [17] L. Peng, P. Liu, X. Feng et al., "Kinetics of heavy metal adsorption and desorption in soil: developing a unified model based on chemical speciation," *Geochimica et Cosmochimica Acta*, vol. 224, pp. 282–300, 2018.
- [18] R. Li, W. Tan, G. Wang et al., "Nitrogen addition promotes the transformation of heavy metal speciation from bioavailable to organic bound by increasing the turnover time of organic matter: an analysis on soil aggregate level," *Environmental Pollution*, vol. 255, Article ID 113170, 2019.
- [19] A. Ertani, A. Mietto, M. Borin, and S. Nardi, "Chromium in agricultural soils and crops: a review," *Water Air and Soil Pollution*, vol. 228, 2017.
- [20] J. Tang, Q. Xue, H. Chen, and W. Li, "Mechanistic study of lead desorption during the leaching process of ion-absorbed rare earths: pH effect and the column experiment," *Environmental Science and Pollution Research*, vol. 24, no. 14, pp. 12918–12926, 2017.
- [21] S. Li, B. Fang, D. Wang, X. Wang, X. Man, and X. Zhang, "Leaching characteristics of heavy metals and plant nutrients in the sewage sludge immobilized by composite phosphorus-bearing materials," *International Journal of Environmental Research and Public Health*, vol. 16, no. 24, p. 5159, 2019.
- [22] J. Qiao, J. Tang, and Q. Xue, "Study on Pb release by several new lixiviants in weathered crust elution-deposited rare earth ore leaching process: behavior and mechanism," *Ecotoxicology and Environmental Safety*, vol. 190, Article ID 110138, 2020.
- [23] H. R. Motaghian and A. R. Hosseini, "Zinc desorption kinetics in wheat (*Triticum Aestivum* L.) rhizosphere in some sewage sludge amended soils," *Journal of Soil Science and Plant Nutrition*, vol. 13, pp. 664–678, 2013.
- [24] H. I. Inyang, A. Onwawoma, and S. Bae, "The Elovich equation as a predictor of lead and cadmium sorption rates on contaminant barrier minerals," *Soil and Tillage Research*, vol. 155, pp. 124–132, 2016.
- [25] D. L. Sparks, "Kinetics of ionic reactions in clay minerals and soils," *Advances in Agronomy*, vol. 38, pp. 231–266, 1986.

- [26] L. Liu, D. Luo, G. Yao et al., "Comparative activation process of Pb, Cd and Tl using chelating agents from contaminated red soils," *International Journal of Environmental Research and Public Health*, vol. 17, no. 2, p. 497, 2020.
- [27] A. G. Caporate and A. Violante, "Chemical processes affecting the mobility of heavy metals and metalloids in soil environments," *Current Pollution Reports*, vol. 2, pp. 15–27, 2016.
- [28] S. A. Zheng, X. Zheng, and C. Chen, "Leaching behavior of heavy metals and transformation of their speciation in polluted soil receiving simulated acid rain," *PLoS One*, vol. 7, Article ID e49664, 2012.
- [29] W. D. Bowman, C. C. Cleveland, L. Halada, J. Hreško, and J. S. Baron, "Negative impact of nitrogen deposition on soil buffering capacity," *Nature Geoscience*, vol. 1, no. 11, pp. 767–770, 2008.
- [30] N. S. Bolan, D. C. Adriano, and D. Curtin, "Soil acidification and liming interactions with nutrient and heavy metal transformation and bioavailability," *Advances in Agronomy*, vol. 78, pp. 215–272, 2003.
- [31] G. Yan, Y. Xing, S. Han, J. Zhang, Q. Wang, and C. Mu, "Long-time precipitation reduction and nitrogen deposition increase alter soil nitrogen dynamic by influencing soil bacterial communities and functional groups," *Pedosphere*, vol. 30, no. 3, pp. 363–377, 2020.
- [32] X.-z. Yuan, Y.-w. Zhang, H. Liu, S. Xiong, B. Li, and W. Deng, "The littoral zone in the Three Gorges Reservoir, China: challenges and opportunities," *Environmental Science and Pollution Research*, vol. 20, no. 10, pp. 7092–7102, 2013.
- [33] J. Tang, Y. P. Zhong, and L. Wang, "Background value of soil heavy metal in the three Gorges reservoir District," *Chinese Journal of Eco-Agriculture*, vol. 16, no. 4, pp. 848–852, 2008, in Chinese.
- [34] C. Ye, S. Li, Y. Zhang, X. Tong, and Q. Zhang, "Assessing heavy metal pollution in the water level fluctuation zone of China's Three Gorges Reservoir using geochemical and soil microbial approaches," *Environmental Monitoring and Assessment*, vol. 185, no. 1, pp. 231–240, 2013.